GaInSb/AlInSb multi-quantum-wells for mid-infrared lasers

M. Yin,[1] G. R. Nash,[2,a)] S. D. Coomber,[3] L. Buckle,[3] P. J. Carrington,[1] A. Krier,[1] A. Andreev,[4] S. J. B. Przeslak,[5] G. de Valicourt,[6] S. J. Smith,[3] M. T. Emeny,[3] and T. Ashley[3]

[1]*Department of Physics, Lancaster University, Lancaster LA1 4YB, United Kingdom*
[2]*QinetiQ, Malvern Technology Centre, Malvern WR14 3PS, United Kingdom and Photonics Group, Department of Electrical and Electronic Engineering, University of Bristol, Bristol BS8 1UB, United Kingdom*
[3]*QinetiQ, Malvern Technology Centre, Malvern WR14 3PS, United Kingdom*
[4]*Department of Physics, Advanced Technology Institute, University of Surrey, Guildford GU2 7XH, United Kingdom*
[5]*Department of Electrical and Electronic Engineering, University of Bristol, Bristol BS8 1UB, United Kingdom*
[6]*Department of Computing and Electronic Systems, University of Essex, Colchester CO4 3SQ, United Kingdom*

(Received 7 July 2008; accepted 1 September 2008; published online 23 September 2008)

Photoluminescence (PL) from GaInSb/AlInSb type I multi-quantum-wells, grown on GaAs, has been investigated as a function of strain in the quantum wells. Luminescence, between 3 and 4 μm, was observed for all samples, with good agreement between the measured and calculated peak emission energies. Analysis of the temperature dependence of the luminescence suggests that population of excited quantum well hole subbands occurs at high temperature, leading to a reduction in the PL signal. Room temperature luminescence was obtained from a sample with ~0.8% strain in the quantum wells. Preliminary results from laser diodes fabricated from companion wafers indicate lasing up to 220 K. © *2008 American Institute of Physics*. [DOI: 10.1063/1.2990224]

Continuing interest in the development of III-V alloys for use in mid-infrared (3–5 μm) light sources and detectors is driven by the extensive range of potential applications in this spectral region, including environmental gas monitoring, noninvasive medical diagnosis, tunable infrared spectroscopy, and free space optical communications.[1] Over the last couple of years, there has been significant progress in laser performance leading to, for example, recent reports of room temperature cw lasing at 3.8 μm from quantum cascade lasers,[2] at 3.75 μm from interband cascade lasers,[3] and at 3.36 μm from compressively strained type 1 quantum wells (QWs).[4] We have also previously reported lasing from simpler double heterostructures[5] and type I multi-quantum-well (MQW) lasers based on the GaInSb/AlGaInSb/AlInSb material system.[6] This material system has the potential advantages of being able to achieve band offsets suitable for electronic confinement and also provide sufficiently high compressive strain for lower threshold laser operation,[7] and we recently reported on the successful realization of mid-infrared coherent emission from MQW diode lasers using this material system grown by molecular beam epitaxy (MBE) on GaAs substrates.[6] However, to realize the advantages of this material system, a greater understanding of the optical properties of these MQWs is required, and in this paper we analyze the photoluminescence (PL) from the GaInSb MQWs in the active region, with the aim of investigating the effect of strain in the QWs on their optical properties. We also report preliminary measurements made on laser diodes fabricated from companion wafers and the materials parameters and theoretical model used to describe the PL results will be later applied to fully understand the properties of these lasers.

Samples were grown by MBE onto semi-insulating GaAs substrates at QinetiQ Malvern. Samples for PL studies consisted of 15 $Ga_rIn_{1-r}Sb$ QWs (nominal thickness 10 nm) with $Al_pGa_qIn_{1-p-q}Sb$ barriers (nominal thickness 20 nm), as shown schematically in Fig. 1(b). For each strain iteration, two additional structures were grown at the same time: a structure consisting of the bottom $Al_xIn_{1-x}Sb$ cladding and $Al_pGa_qIn_{1-p-q}Sb$ barrier only and a complete laser structure[6] containing two QWs. The composition of the different layers in the MQW samples was determined by performing high resolution x-ray diffraction (XRD) measurements on all the structures grown at each strain iteration and by determining

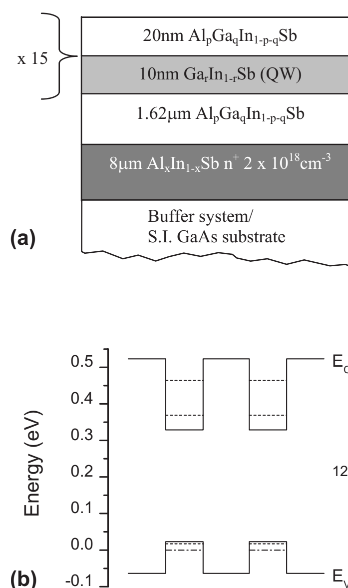

FIG. 1. Schematic cross section (a) showing the generic structure of the samples and (b) the calculated energy band diagram of Sample A under zero net bias and at 12 K. The dashed lines correspond to the two lowest energy electron and hole subbands.

a)Electronic mail: grnash@qinetiq.com.

 © 2008 American Institute of Physics

Downloaded 30 Mar 2009 to 131.227.178.132. Redistribution subject to AIP license or copyright; see http://apl.aip.org/apl/copyright.jsp

TABLE I. Summary of the properties of the four PL samples.

Sample	$Al_xIn_{1-x}Sb$ cladding	$Al_pGa_qIn_{1-p-q}Sb$ barriers	$Ga_rIn_{1-r}Sb$ QWs	QW strain (%)	Peak PL energy (meV)	E1-H1 (meV) at 12 K	E1-CB (meV) at 12 K	H1-VB (meV) at 12 K
A	$x=0.30$	$p=0.13$, $q=0.17$	$r=0.19$	0.64	364	352	154	81
B	$x=0.28$	$p=0.14$, $q=0.15$	$r=0.18$	0.71	373	378	152	88
C	$x=0.37$	$p=0.19$, $q=0.18$	$r=0.22$	0.86	383	383	237	121
D	$x=0.43$	$p=0.21$, $q=0.20$	$r=0.25$	0.94	396	403	260	130

the QW thickness using transmission electron microscopy. The percentage strain in the QWs is defined as $[(a_{\|}-a_0)/a_0]\times 100$, where a_0 where is the cubic (unstrained) lattice constant and $a_{\|}$ is the parallel (in-plane) lattice constant. a_0 was obtained from simulation of the (400) rocking curve for the 15 period barrier/QW structure and $a_{\|}$ from XRD measurement of the barrier lattice parameters, i.e., a fully strained system was assumed with $a_{\|}$(barrier) equal to $a_{\|}$(QW). This assumption is consistent with the sharpness of the peaks observed in the rocking curve. The composition of each PL sample is summarized in Table I. In the PL experiment, an Ar+ ion laser (514 nm) was used to excite the samples with a maximum excitation power density at the sample of 2 W/cm^2. The sample temperature was varied between 4 and 300 K using a continuous flow He cryostat system. The resulting PL emission was dispersed with a 0.3 m grating monochromator and detected using a 77 K InSb photodiode and a conventional lock-in amplifier. The monochromator resolution was typically 2 nm.

Figure 2 shows the PL intensity measured at 12 K for each of the four samples. The maximum in PL intensity was estimated to occur at 364, 373, 383, and 396 meV for samples A, B, C, and D, respectively. The corresponding energies at which the maximum PL intensity was obtained is plotted as a function of the QW strain in the inset of Fig. 2, and these energies show a monotonic dependence on the QW strain. An eight band $k\cdot p$ model was used to calculate the energy levels within the QW with strain taken into account[8] and material parameters taken from Ref. 9 giving values of the E1-H1 transition as 352, 378, 383, and 403 meV for samples A, B, C, and D, respectively, in close agreement to the measured values, as summarized in Table I.

The full width at half maximum (FWHM) of the PL signal at 12 K was estimated to be ~14, 31, 18, and 38 meV for samples A, B, C, and D. These values are of the same order as those obtained, for example, from GaInAsSb–AlGaAsSb samples grown on GaSb,[10] indicating that growth of high quality AlGaInSb/GaInSb QWs is possible on lattice mismatched GaAs substrates, offering potential advantages in terms of cost and integration. However, the surface morphology of sample D was not as good as that of the other samples, as the growth process is not yet fully optimized for the highest Al compositions. This may explain the relatively large FWHM obtained from this sample (the reason for the relatively high FWHM obtained for sample B is unclear at this stage). The PL intensity was measured up to 180 K for all samples and the integrated PL intensity was observed to decrease with increasing temperature for all samples. The PL signal from sample C was measured up to room temperature, and in Fig. 3 the temperature dependence of the integrated PL intensity is plotted as a function of temperature. The inset is the Arrhenius plot of the same data. There appears to be a regime with an activation energy of ~40 meV at high temperatures, and a regime at low temperatures where the activation energy asymptotically approaches 0 meV. Similar behavior is observed in the other samples, and also in other material systems, where the high temperature activation energy is thought to correspond to the thermally activated escape of carriers from the QW.[11] However, in our case, this activation energy is much smaller than the energy difference

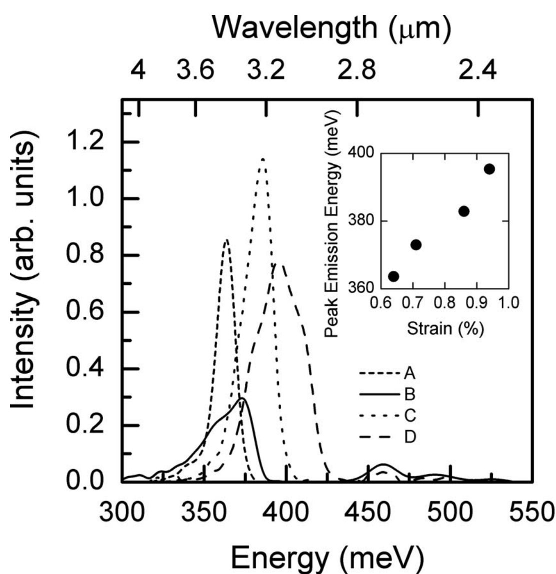

FIG. 2. Measured PL signal at 12 K from MQW samples A, B, C, and D. The inset is a plot of the energy at which the maximum PL signal occurs, together with the integrated PL intensity, as a function of QW strain (lines are guides to the eye).

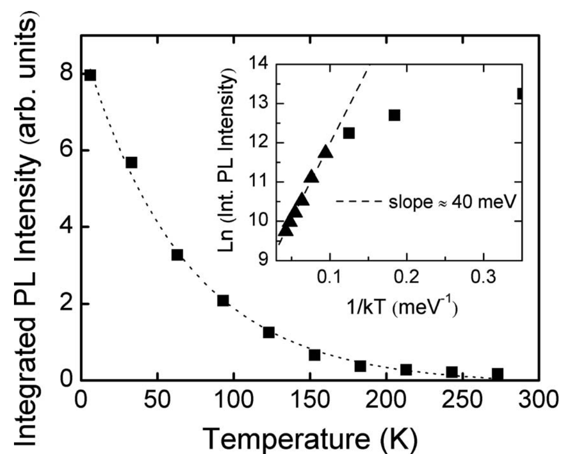

FIG. 3. Temperature dependence of the integrated PL signal from sample C (the line is a guide to the eye only). The same experimental data is shown in an Arrhenius plot in the inset, with a linear least-squares fit to the data at high temperatures.

Downloaded 30 Mar 2009 to 131.227.178.132. Redistribution subject to AIP license or copyright; see http://apl.aip.org/apl/copyright.jsp

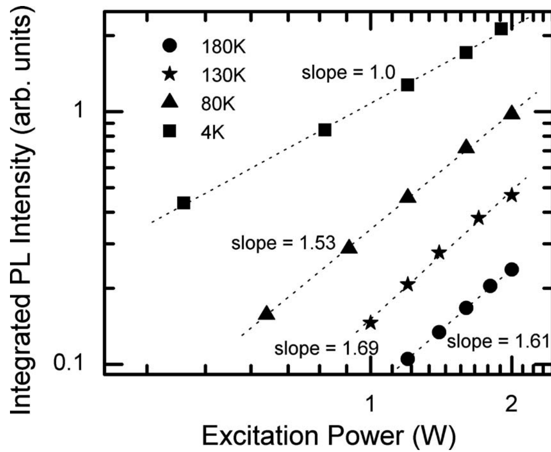

FIG. 4. Integrated PL signal from sample D plotted as a function of incident laser power (P_{exc}), on log scales as a function of temperature. The dotted lines are linear least-squares fits to the data.

between the lowest energy QW electron (E1) subband and the barrier conduction band, and the energy difference between the lowest energy QW hole (H1) subband and the barrier valence band (which is greater than ~100 meV in all samples in each case, as shown in Table I). However, as the temperature increases, higher hole subbands could start to become populated. The value of activation energy extracted is consistent with the calculated energy separation of the lowest and first excited hole subbands. Since there is no clear evidence of transitions other than E1 to H1 in the measured spectra shown in Fig. 2, we assume that most of the PL signal originates from this transition and that the other subbands are not populated under these pumping conditions. Greater population of the higher energy hole subbands could lead to a reduced PL signal in several ways. The reduced population of the lowest hole subband leads to reduced E1-H1 recombination, the optical strength of the transitions between E1 to excited hole subbands is weaker, and finally additional nonradiative Auger processes become available. Further modeling is underway to determine which of these mechanisms is dominant.

In Fig. 4, the integrated PL intensity (for sample D) is plotted as a function of laser excitation power. The integrated PL intensity is plotted on a log-log scale, together with linear fits, showing that the integrated PL intensity I_{PL} is related to the excitation intensity I_{ex} by $I_{PL} \propto I_{ex}^{\alpha}$, where α is given by the slope of linear fits shown in the inset, as predicted from analysis of the appropriate rate equations.[12] In this case, the value of α was found to be 1, 1.53, 1.69, and 1.61 at 4, 80, 130, and 180 K, respectively, suggesting that at low temperature the luminescence is dominated by exciton recombination,[12] and at high temperatures it is dominated by a mixture of free carrier recombination and exciton recombination. Similar behavior was exhibited by the other samples, with values of α at 4/80 K for samples A, B, and C of 1.39/1.89, 1.12/1.69, and 1.19/1.61, respectively.

Finally, a number of laser diodes were fabricated from each of the full laser structures L1, L2, L3, and L4, the composition of which are summarized in Table II. Preliminary measurements at 100 K have yielded average threshold current densities of 650 A/cm^2, 220 A/cm^2, 484 A/cm^2, and 2.7 kA/cm^2, with lasing observed at wavelengths of 3.41, 3.44, 3.23, and 2.96 μm, respectively for L1, L2, L3, and L4. Clear threshold currents were observed in the measured light-current characteristics up to temperatures of 161, 208, 219, and 151 K for samples L1, L2, L3, and L4, respectively. As for the PL samples, the surface morphology of sample L4 was not as good as that of the other samples, and work is underway to optimize the growth process to allow the fabrication of lasers with higher strain. Recent room temperature lasing from GaSb based type 1 structures[4] was achieved with 1.5% strain in the QWs, as compared to only ~0.8% for sample L3, suggesting that there is scope for significant improvement to these lasers. Further experiments are underway to fully characterize these devices and full details of the device processing and characterization and comparison with theoretical modeling will appear elsewhere.[13]

TABLE II. Summary of the properties of the four laser samples.

Sample	$Al_xIn_{1-x}Sb$ cladding	$Al_pGa_qIn_{1-p-q}Sb$ barriers	$Ga_rIn_{1-r}Sb$ QWs	QW strain (%)
L1	$x=0.30$	$p=0.09$, $q=0.16$	$r=0.18$	0.55
L2	$x=0.30$	$p=0.11$, $q=0.17$	$r=0.19$	0.62
L3	$x=0.38$	$p=0.15$, $q=0.19$	$r=0.22$	0.78
L4	$x=0.41$	$p=0.18$, $q=0.21$	$r=0.25$	0.81

In conclusion, we have investigated the PL characteristics of GaInSb/AlGaInSb type I MQWs, grown onto GaAs, as a function of increasing strain. Luminescence was observed for all samples, with room temperature luminescence observed for the sample with only ~0.9% strain in the QWs, offering the prospect of exploiting this material system to realize room temperature laser diodes emitting in the important 3–4 μm region. Analysis of the temperature dependence of the luminescence suggests that population of excited QW hole subbands occurs at high temperature, leading to a reduction in the PL signal. Work is now underway to fully investigate the properties of laser diodes containing similar QWs in the active region.

This work was supported by the UK Technology Strategy Board Technology Programme. The authors wish to thank Gerald Williams and Andrew Keir for undertaking the TEM and XRD measurements, respectively.

[1]X. Marcadet, C. Renard, M. Carras, M. Garcia, and J. Massies, Appl. Phys. Lett. **91**, 161104 (2007).
[2]J. S. Yu, A. Evans, S. Slivken, S. R. Darvish, and M. Razeghi, Appl. Phys. Lett. **88**, 251118 (2006).
[3]M. Kim, C. L. Canedy, W. W. Bewley, C. S. Kim, J. R. Lindle, J. Abell, I. Vurgaftman, and J. R. Meyer, Appl. Phys. Lett. **92**, 191110 (2008).
[4]L. Shterengas, G. Belenky, T. Hosoda, G. Kipshidze, and S. Suchalkin, Appl. Phys. Lett. **93**, 011103 (2008).
[5]M. Yin, A. Krier, R. Jones, and P. J. Carrington, Appl. Phys. Lett. **91**, 101104 (2007).
[6]G. R. Nash, S. J. Smith, S. D. Coomber, S. Przeslak, A. Andreev, P. Carrington, M. Yin, A. Krier, L. Buckle, M. T. Emeny, and T. Ashley, Appl. Phys. Lett. **91**, 131118 (2007).
[7]See, for example, L. Shterengas, G. Belenky, M. V. Kisin, and D. Donetsky, Appl. Phys. Lett. **90**, 011119 (2007).
[8]A. D. Andreev, E. P. O'Reilly, A. R. Adams, and T. Ashley, Appl. Phys. Lett. **78**, 2640 (2001).
[9]I. Vurgaftman, J. R. Meyer, and L. R. Ram-Mohan, J. Appl. Phys. **89**, 5815 (2001).
[10]G. Rainò, A. Salhi, V. Tasco, R. Intartaglia, R. Cingolani, Y. Rouillard, E. Tournié, and M. De Giorgi, Appl. Phys. Lett. **92**, 101931 (2008).
[11]J. Pannekamp, S. Weber, W. Limmer, and R. Sauer, J. Lumin. **85**, 37 (1999), and references therein.
[12]J. E. Fouquet and A. E. Siegman, Appl. Phys. Lett. **46**, 280 (1985).
[13]G. R. Nash, S. J. B. Przeslak, S. J. Smith, G. de Valicourt, L. Buckle, S. D. Coomber, A. Andreev, P. Carrington, M. Yin, A. Krier, L. Buckle, M. T. Emeny, and T. Ashley, Appl. Phys. Lett. (submitted).

Downloaded 30 Mar 2009 to 131.227.178.132. Redistribution subject to AIP license or copyright; see http://apl.aip.org/apl/copyright.jsp